



## LJMU Research Online

**Gonzalez-Prieto, I, Zoric, I, Duran, MJ and Levi, E**

**Constrained Model Predictive Control in Nine-phase Induction Motor Drives**

<http://researchonline.ljmu.ac.uk/id/eprint/11047/>

### Article

**Citation** (please note it is advisable to refer to the publisher's version if you intend to cite from this work)

**Gonzalez-Prieto, I, Zoric, I, Duran, MJ and Levi, E (2019) Constrained Model Predictive Control in Nine-phase Induction Motor Drives. IEEE Transactions on Energy Conversion. ISSN 0885-8969**

LJMU has developed **LJMU Research Online** for users to access the research output of the University more effectively. Copyright © and Moral Rights for the papers on this site are retained by the individual authors and/or other copyright owners. Users may download and/or print one copy of any article(s) in LJMU Research Online to facilitate their private study or for non-commercial research. You may not engage in further distribution of the material or use it for any profit-making activities or any commercial gain.

The version presented here may differ from the published version or from the version of the record. Please see the repository URL above for details on accessing the published version and note that access may require a subscription.

For more information please contact [researchonline@ljmu.ac.uk](mailto:researchonline@ljmu.ac.uk)

<http://researchonline.ljmu.ac.uk/>

# Constrained Model Predictive Control in Nine-phase Induction Motor Drives

Ignacio Gonzalez-Prieto, Ivan Zoric, Mario J. Duran, Emil Levi, *Fellow, IEEE*

**Abstract**— The advent of powerful digital signal processors (DSPs) has recently permitted the real-time implementation of model predictive control (MPC) in high-performance electric drives. Nevertheless, the use of MPC together with multiphase systems is increasingly challenging as the number of phases gets higher. On the positive side, the redundancy provided by the extra phases also opens the possibility to further optimize the control action. This work describes the implementation of MPC for nine-phase drives using a three-step approach with an initial discarding of the switching states, a dynamic selection of the voltage vectors using hard constraints (HCs), and an improved performance including soft constraints (SCs). Experimental results confirm the ability of the proposed MPC to highly reduce the computational burden and switching frequency, while maintaining satisfactory steady-state and dynamic performance.

**Index Terms**— Multiphase drives, induction motors, model predictive control.

## I. INTRODUCTION

Model predictive control (MPC) has been recently declared a promising candidate to replace some standard controller solutions in high-performance drives (e.g., in field oriented control, [1-7]). The finite-control set type (simply termed MPC in what follows for simplicity) has been compared in literature with other conventional techniques both in three-phase [8-10] and multiphase [11-13] systems. The differences between MPC and linear controllers that include a modulation stage are detailed in [8], while experimental results that compare both approaches are included in [9-10] for three-phase drives, in [11-12] for healthy operation of multiphase drives and in [13] for faulty operation of multiphase drives. MPC is well-known to provide fast dynamic response and high flexibility to easily include additional restrictions. In addition, it offers a simple control structure with no need for a modulation stage (this being similar to direct torque control). On the other hand, some of the disadvantages include a higher computational cost and higher current ripple compared to other control approaches such as the field-oriented control (FOC) with PI current control [8-13].

The use of MPC to regulate electric drives has only become feasible recently thanks to the ever-increasing power of digital signal processors. The computational cost is however directly dependent on the number of iterations and consequently it is

a function of the number of levels and phases of the power converter [2-4]. In standard two-level three-phase systems there are only 8 switching states, but in general an  $m$ -level  $n$ -phase system provides  $m^n$  possibilities (e.g. in a two-level nine-phase voltage source converter (VSC) there are 512 different switching states). A comparison of the execution times for five-phase induction motor drives reveals that the computational cost of MPC is much higher than in other conventional techniques such as direct torque control (DTC) [14]. This problem is further exacerbated in nine-phase systems because the number of iterations is 16 times higher than in five-phase drives, and the predictive model also has to deal with more subspaces. Consequently, the first motivation of this work was to implement for the first time a finite-control set MPC strategy in nine-phase electric drives, including some simplifications to help the real time control realisation.

Even with the current DSP technology, implementation of MPC is still challenging for multilevel/multiphase systems. This disadvantage is inherently present due to the additional degrees of freedom, but at the same time it can be seen as an opportunity to optimize the control performance. While in two-level three-phase systems the control action is much restricted, multiphase systems offer many different switching states with the same or similar voltage production [15-17]. Although some decrease in the considered total number of states might be mandatory to alleviate the computational burden, an intelligent selection of the proper voltage vector can also highly reduce the switching frequency. Hence, the second motivation of this work was to explore how much MPC could be optimized regarding switching frequency reduction, by taking advantage of the inherent redundancy of nine-phase systems.

Initial works on MPC for six-phase drives directly reduced the considered voltage vector number according to their size in the different subspaces after the vector space decomposition (VSD). Discarding some vectors a priori directly reduces the number of iterations and the computational cost (e.g. in [18] only 13 out of 64 switching states were evaluated). Focusing on the number of commutations per sampling period rather than the size of the voltage vectors, a dynamic selection of the switching possibilities with hard constraints (HCs) was also proposed in [19] for six-phase drives. This helped to reduce even more the number of iterations per sampling period. Following the idea of selecting those switching states that commute less, by using soft constraints, a modification of the cost function was suggested in [20] for three-phase multilevel VSCs.

Although most of the work on MPC has been restricted to three-, five- and six-phase drives [1-4,6-20], industry applications of multiphase machines often use multiple three-phase arrangements with a number of phases higher than six

---

This work was supported by the Spanish Ministry of Science and Innovation under Project ENE2014-52536-C2-1-R

I. Gonzalez-Prieto and Mario J. Duran are with the Dept. of Electrical Engineering, University of Malaga, C/ Doctor Ortiz Ramos S/N, 29071 Malaga, Spain (e-mail: [ignaciogp87@gmail.com](mailto:ignaciogp87@gmail.com) and [mjduran@uma.es](mailto:mjduran@uma.es)).

I. Zoric is with Dyson, Tetbury Hill, Malmesbury SN16 0RP Wiltshire, U.K. (e-mail: [ivanzoric497@gmail.com](mailto:ivanzoric497@gmail.com)).

E. Levi is with the Faculty of Engineering and Technology, Liverpool John Moores University, Liverpool L3 3AF, U.K. (e-mail: [e.levi@ljmu.ac.uk](mailto:e.levi@ljmu.ac.uk)).

[21]. It is worth noting that in high-power applications the use of multiple three-phase converters in parallel is already a common procedure, so the change to a multi three-phase drive only requires a different stator winding topology in the motor/generator [21]. More specifically, the area of nine-phase drives has shown a significant growth in recent times [22–26]. The study of MPC together with nine-phase systems is however practically nonexistent in literature. The only work that follows a predictive approach for nine-phase drives can be found in [26], but it deals with symmetrical flux-switching permanent magnet machines and a specific version of MPC that includes space vector pulse width modulation (SVPWM). Consequently, the option to apply hard and soft constraints to reduce the effective switching frequency does not exist. However, nine-phase systems offer a higher number of switching states; hence, it is in principle reasonable to expect that the inherently discrete nature of MPC can benefit from the additional redundancy.

This work aims to investigate the possibilities for real-time implementation and optimization of finite control-set MPC for asymmetrical nine-phase induction motor drives, including vector discarding strategies and the inclusion of hard/soft constraints. Compared to five- and six-phase systems, the number, location and mapping of the voltage vectors in nine-phase systems are completely different and provide a higher degree of redundancy. Even though the problem becomes more complex, it is shown here that the optimization can also be more effective. The most important contributions of this paper are believed to be:

- The analysis of the available voltage vectors in nine-phase systems that allows discarding some of the switching states.
- The analysis of hard constraints (HCs) that dynamically select the most suitable switching states for each sampling period.
- The impact of soft constraints (SCs) that reduce the effective switching frequency with a low impact on the control performance.
- The evaluation of the MPC after vector discarding and inclusion of the HCs and SCs, with extensive experimental results that confirm the possibility to optimize the nine-phase drive performance.

The aforementioned contributions lead to two main novel advances: *i*) it is confirmed that the real time implementation of finite-control set MPC is feasible in nine-phase electric drives if a smart pre-selection of the suitable switching states is performed and *ii*) it is quantitatively verified that the inherent redundancy of nine-phase systems allows a significant optimization of MPC by proper combination of HCs and SCs.

The paper is structured as follows. Sections II and III review the background of nine-phase systems and MPC, respectively. Section IV analyzes the available switching states and selects a subset of voltage vectors (initial discarding) and section V describes the implementation of hard and soft constraints. Section VI experimentally tunes the parameters for the HCs and SCs and verifies the goodness of the proposed MPC strategy. Conclusions are finally summarized in section VII.

## II. NINE-PHASE INDUCTION MOTOR DRIVE

The drive under consideration includes an asymmetrical nine-phase induction machine with distributed windings supplied from a nine-leg bridge two-level (VSC) that is connected to a single dc-link (Fig. 1). The machine has three sets of three-phase windings which are labelled  $a_1b_1c_1$ ,  $a_2b_2c_2$  and  $a_3b_3c_3$ , and are spatially shifted by  $20^\circ$ . Since the machine is configured with three isolated neutral points, the vector space decomposition (VSD) maps the nine-phase dimensional space into one  $\alpha$ - $\beta$  plane, two secondary planes (typically termed  $x_1$ - $y_1$  and  $x_2$ - $y_2$  [16]) and three non-excitable zero-sequence components. The distributed-winding arrangement allows neglecting spatial harmonics; hence the production of flux/torque is confined to the first ( $\alpha$ - $\beta$ ) plane and the secondary currents are responsible only for additional stator copper losses.

While the model of the machine is very similar to five- and six-phase systems (for further details see [16–18]), the available voltage vectors are completely different in terms of the total number, location and size. The switching combinations can be defined by the switching vector:

$$\bar{S} = [S_{a1} S_{b1} S_{c1} S_{a2} S_{b2} S_{c2} S_{a3} S_{b3} S_{c3}], \quad (1)$$

where the switching function  $S_k = 1$  if the phase is connected to the positive rail of the VSC and  $S_k = 0$  otherwise.

The dc-link voltage ( $V_{dc}$ ) and the switching states from (1) provide  $2^9 = 512$  values of the leg voltages ( $V_k$ ):

$$V_k = V_{DC} \cdot S_k, \quad (2)$$

which in turn give different phase voltages ( $v_k$ ):

$$v_k = \frac{8}{9}V_k - \frac{1}{9}\sum_{i=1, i \neq k}^9 V_i \quad (3)$$

The application of the generalized Clarke transformation finally provides  $2^9 = 512$  voltage vectors in the VSD domain. Compared to the five- and six-phase cases, the voltage vectors of the nine-phase VSC are more abundant, disperse and mapped in more planes. Furthermore, there is a higher degree of redundancy and hence room for MPC optimization because different switching states create the same output voltages. Section IV further explores the nature of the available voltage vectors and the possibility to discard those providing unsuitable values for the machine operation.

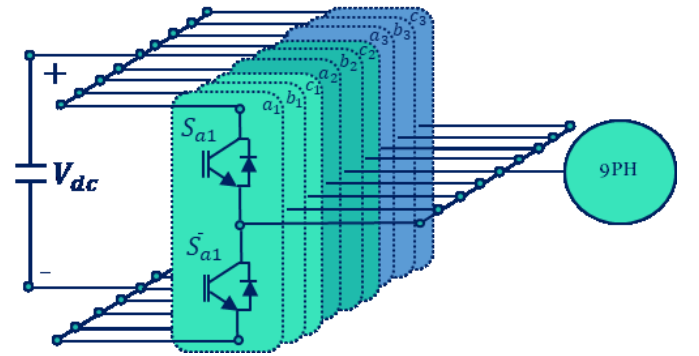


Fig. 1: Asymmetrical nine-phase induction motor supplied from two-level nine-phase VSC.

### III. MODEL PREDICTIVE CONTROL OF NINE-PHASE INDUCTION MOTOR DRIVES

Numerous attempts to improve standard high-performance control techniques for electric drives have appeared in recent times. One of the most recent and promising candidates is the model predictive control (MPC). MPC firstly uses a predictive model to estimate the future states of the drive and then selects the most suitable control output for application in the next sampling period. In this work the MPC approach replaces the current control loops, while maintaining the speed loop with a PI controller and the standard indirect field-oriented control [21] (see Fig. 2). Since this works exclusively deals with the healthy operation of the nine-phase electric drive, the  $x$ - $y$  current references are set to zero for the sake of efficiency.

In its finite control-set full version, MPC performs one prediction per switching state, resulting in  $2^9 = 512$  iterations in the drive topology shown in Fig. 1. As in direct torque control (DTC), the selected switching state is applied during the whole sampling period without the need for pulse width modulation (PWM). Each iteration  $k$  evaluates a cost function  $J_k$  that minimizes the overall current tracking error  $e$ :

$$J_k = K_{\alpha\beta} \cdot e_{\alpha\beta} + K_{xy1} \cdot e_{xy1} + K_{xy2} \cdot e_{xy2}$$

$$e_{\alpha\beta} = (i_{\alpha}^* - \hat{i}_{\alpha})^2 + (i_{\beta}^* - \hat{i}_{\beta})^2$$

$$e_{xy1} = (i_{x1}^* - \hat{i}_{x1})^2 + (i_{y1}^* - \hat{i}_{y1})^2$$

$$e_{xy2} = (i_{x2}^* - \hat{i}_{x2})^2 + (i_{y2}^* - \hat{i}_{y2})^2,$$
(4)

and selects the switching state that minimizes the cost function. Coefficients  $K_{ij}$  are the weighting factors. The predictive model is obtained using the Euler discretization technique for the machine equations in the stationary reference frame, these being an extension of the approach in [5], where some further details about the predictive model can be found. Although the optimal case is ensured by considering all 512 iterations, the computational cost can be alleviated by considering a subset of the switching states, as it is justified in the next section.

### IV. ANALYSIS OF THE VOLTAGE VECTORS

Once the nine-phase system and the control approach have been briefly described in the preceding two sections, the next step is to decide how many voltage vectors will be used in the iterative process shown in Fig. 2. The decision is a trade-off between loss of optimality and the feasibility for real time implementation. The voltage vectors are obtained by calculating the phase voltage associated to each switching state and then applying the generalized Clarke transformation to obtain the  $\alpha$ - $\beta$  and  $x$ - $y$  voltage components [21] (Fig. 3).

One of the well-known disadvantages of MPC is the computational cost, and this shortcoming is particularly noticeable in the case of two-level nine-phase VSC of Fig. 1, where the number of switching combinations is 64 times higher than in two-level three-phase converters ( $2^9 = 512$  states compared to  $2^3 = 8$ ). Although considering all 512 voltage vectors ensures optimality (optimal model predictive control will be termed MPC512 from now on), it is possible to discard vectors that are not selected by the MPC algorithm and in this way alleviate the computational effort and ease the real time implementation. This discarding can be done on the basis of the contribution of each switching state to the principal ( $\alpha\beta$ ) and secondary ( $xy$ ) planes.

Voltage vectors that mostly contribute to the  $xy$  plane instead of the  $\alpha\beta$  plane will not be selected by the MPC algorithm even if they are included in the iterative process, because they would generate little flux/torque and huge stator copper losses. In order to quantify the contribution of each switching state to the principal and secondary planes, let us define an index that provides the ratio of  $\alpha\beta$  to  $xy$  voltage generation:

$$R_{\alpha\beta} = \frac{|v_{\alpha\beta}|}{\sqrt{|v_{xy1}|^2 + |v_{xy2}|^2}} \quad (5)$$

where  $|v_{\alpha\beta}|$ ,  $|v_{xy1}|$  and  $|v_{xy2}|$  are the amplitude/modulus of the voltage vectors in the different planes after the vector space decomposition.

Except for some intermediate points, most of the 512 voltage vectors are located in 10 sets with 18 vectors each, that will be termed C1 to C10 in descending order of  $|v_{\alpha\beta}|$ . For the sake of illustration, Fig. 3 highlights sets C1 (Fig. 3a) and C6 (Fig. 3b) with aquamarine points among the 512 voltage vectors (marked with red points).

The amplitudes of the ten groups in the different planes ( $|v_{\alpha\beta}|$ ,  $|v_{xy1}|$  and  $|v_{xy2}|$ ) shown in Fig. 3 are summarized in Table I together with the  $\alpha\beta$  contribution ratio ( $R_{\alpha\beta}$ ) and the percentage of this ratio (taking C1 as the base value). The most favorable voltage vectors are those located in set C1 since they provide maximum  $\alpha\beta$  contribution and low contribution to the secondary planes ( $R_{\alpha\beta} = 3.3$ ). On the contrary, sets C7 to C10 can be discarded a priori because they mostly contribute to  $xy$  planes rather than to flux/torque production (the value of  $R_{\alpha\beta}$  is less than 10% in C7-C10).

Aiming to sweep the full voltage range, some sets from C2 to C6 can be selected for MPC evaluation. Even if they contribute less than C1 to the  $\alpha\beta$  production, their selection can improve the drive operation when the required voltage in the  $\alpha\beta$  plane is small (e.g. low speed operation), because the voltage provided by the set C1 might be excessive. For this purpose, groups C3 and C6 can be selected in order to cover the medium and low voltage regions. Set C2 is discarded because it is too close to the set C1 (with higher value of  $R_{\alpha\beta}$ ), group C5 is discarded because its contribution is only 15% compared to C1, and set C3 is finally a preferred choice compared to C4 because the  $xy$  plane contribution is lower.

The selection of C1, C3 and C6 as the switching states to be included in the iterative process of MPC reduces the number of iterations 4 times (from 512 to 127), easing in this manner the real-time implementation without affecting optimality (see experimental results in section VI for confirmation). MPC iterating only switching states from groups C1, C3 and C6 will be termed MPC127 from now on.

### V. HARD AND SOFT CONSTRAINTS

Even though the number of available vectors has been reduced to one fourth in the previous section, there are still many vectors that are relatively close or even redundant (e.g. vectors 321 and 467 provide exactly the same phase voltages). Consequently, it is convenient to distinguish between vectors that will provide the same or similar phase voltages/currents. For the sake of efficiency, MPC should promote those vectors

that provide lower number of commutations in a certain sampling period, and this can be done by the inclusion of soft or hard constraints.

Soft constraints (SCs) do not discard any vector a priori, but penalize the applications of vectors that provide higher switching frequency. This can be simply implemented by including a new term in the cost function that favors the voltage vectors that involve fewer commutations:

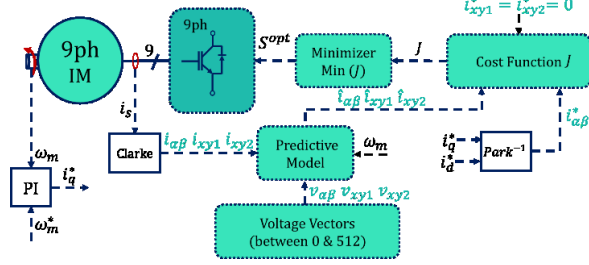


Fig. 2. Scheme of the finite control set MPC strategy for the nine-phase induction motor drive.

TABLE I

AMPLITUDE AND CONTRIBUTION RATIO OF THE VOLTAGE VECTORS IN EACH SUBSPACE GROUPED IN SETS C1 TO C10 AND NORMALIZED WITH  $V_{dc}$

Set	C1	C2	C3	C4	C5	C6	C7	C8	C9	C10
$ v_{\alpha\beta}  \cdot 10^2$	64	56	42	34	30	22	20	15	12	8
$ v_{xy1}  \cdot 10^2$	15	20	8	42	56	22	30	12	64	34
$ v_{xy2}  \cdot 10^2$	12	30	34	8	20	22	56	64	15	42
$R_{\alpha\beta}$	3.3	1.5	1.2	0.8	0.5	0.7	0.3	0.23	0.18	0.15
%	100	46	36	24	15	21	9	7	5	4

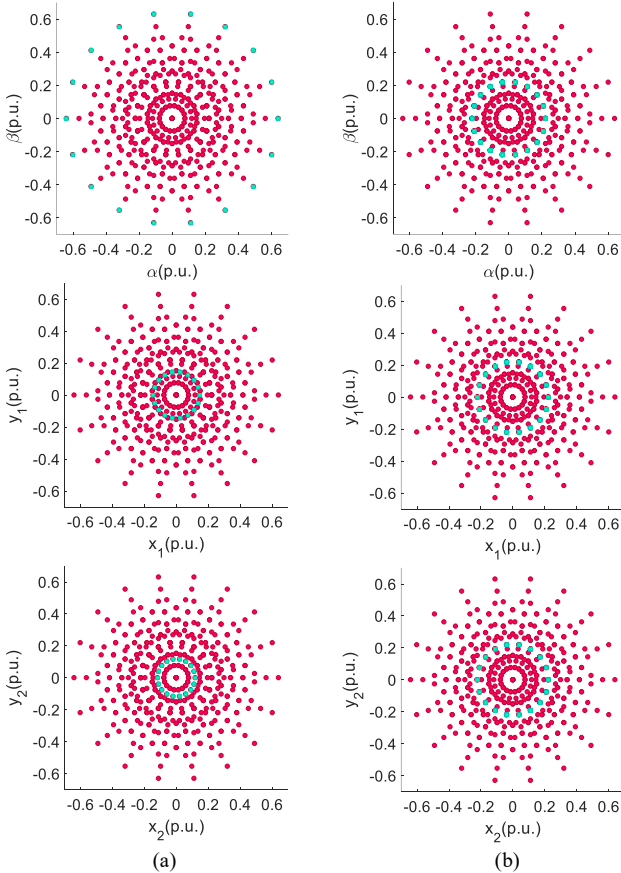


Fig. 3. Voltage vectors in the  $\alpha\beta$  plane (top plots),  $x_1y_1$  plane (middle plots) and  $x_2y_2$  plane (bottom plots). Sets C1 (left plots) and C6 (right plots) highlighted in aquamarine color.

$$J_k = K_{\alpha\beta} \cdot e_{\alpha\beta} + K_{xy1} \cdot e_{xy1} + K_{xy2} \cdot e_{xy2} + K_{sw} \cdot C_{jk}, \quad (6)$$

where  $K_{sw}$  is a switching weighting factor and  $C_{jk}$  is the number of commutations of switching state  $k$  in the sampling period  $j$ :

$$C_{jk} = \sum_{i=1}^9 |S_{i|j} - S_{i|(j-1)}|, \quad (7)$$

where  $S_{i|j}$  and  $S_{i|(j-1)}$  are the switching states of leg  $i$  in the current ( $j$ ) and previous sampling period ( $j-1$ ), respectively.

The unconstrained MPC can be obtained by setting  $K_{sw} = 0$ . Alternatively, the value of this weighting factor can be increased to gradually promote those switching states that provide satisfactory current tracking with lower switching frequency. The soft approach provides a fine tuning because  $K_{sw}$  is a parameter whose value can be set continuously, but, as a main drawback, it does not reduce the computational cost because all 127 switching states need to be evaluated in each sampling period.

Alternatively, one can use hard constraints (HCs) and directly discard in advance those switching states that commute more. The number of VSC legs that switch in a certain sampling period is given by (7) and one can set a threshold  $C_{sw}$  to avoid vectors with a value of  $C_{jk}$  greater than  $C_{sw}$ . In pseudocode:

```

for k = 1 to 127
  if  $C_{jk} \leq C_{sw}$ 
    Iterate MPC
  end
end

```

(8)

If  $C_{sw} \geq 9$  then all 127 voltage vectors from sets C1, C3 and C6 are included in the iterative process of Fig. 2 and for  $C_{sw} = 1$  only 9 vectors among the 127 would be considered. Intermediate values from 8 to 2 gradually reduce the number of voltage vectors that are evaluated by the MPC algorithm.

The main advantage of the hard constraint approach is the reduction of the computational burden caused by the reduced number of MPC iterations. Nevertheless, it is a less flexible approach because switching states that do not comply with restriction  $C_{jk} \leq C_{sw}$  are discarded a priori even if they provide a satisfactory current tracking error. On the contrary, the soft approach evaluates switching states with  $C_{jk} \leq C_{sw}$  and has the ability to select them only in cases when the satisfactory current tracking compensates for the higher number of commutations. For this reason, it is expected that the hard approach will effectively reduce the computational cost whereas the soft approach will find a better balance between low switching frequency and low total harmonic distortion (THD) of phase currents. As a logical consequence, the combination of soft and hard restrictions should maintain a suitable current tracking and power quality with a significant reduction of both the computational burden and the effective switching frequency. This assumption is confirmed next with experiments.

## VI. EXPERIMENTAL RESULTS

### A. Experimental Rig

An experimental setup based on an asymmetrical nine-phase induction machine is employed to validate the goodness of the proposed method. The stator of a three-phase machine has been rewound to create an asymmetrical nine-phase winding. The rewound machine parameters are listed in Table II (index  $l$  denotes leakage inductances, index  $m$  magnetizing inductance,

while index  $L_m$  stands for the mutual leakage inductance;  $P$  is the number of pole pairs of the machine). During the tests, the machine is used in a configuration with three neutral points. The nine-phase machine is mechanically coupled to a dc machine by a Magtrol TM 210 torque meter. The dc machine can be configured in two different operating modes. In the first of these modes, the dc machine is supplied by a Sorensen SGI600/25 dc supply, which can operate in a constant current mode. This enables constant torque operation of the dc machine. In the second operating mode, the dc machine is connected to a passive load and therefore the dc machine operates like a generator.

The nine-phase machine is supplied using two custom-made inverters, based on Infineon FS50R12KE3 IGBT modules. The inverter dc-link voltage (300 V) is provided by Spitzenberger & Spies linear amplifier PAS2500. A dSPACE ds1006 platform is employed to implement the proposed control method and to realize the measurements of the control variables. During all tests, a sampling frequency of 10 kHz is employed and an ADC board is used to acquire phase currents measured by inverter's internal LEM sensors, while an incremental encoder board provides speed and position by capturing signals from an incremental encoder, mounted on the shaft of the nine-phase machine. The experimental test bench is shown in Fig. 4, where its major parts are labelled.

### B. Experimental Results

The MPC is generally regarded as a time-consuming control approach when compared to other conventional strategies [13]. This problem becomes worse and worse as the number of switching states grow. It is fair to say immediately that the full MPC with 512 iterations cannot be implemented in real time using the previously described experimental platform. However, if the number of iterations is reduced down to 127, the application of MPC becomes feasible. Hence, the state discarding, described in section IV, is mandatory in this case. All results shown next will be based on the standard case of MPC with 127 iterations together with soft and hard constraints, and will be classified into three sets of tests:

TABLE II  
ASYMMETRICAL NINE-PHASE INDUCTION MACHINE PARAMETERS

$R_{\alpha\beta s} = R_{xy s}$	5.3 $\Omega$	$R_r$	2.0 $\Omega$
$L_{\alpha\beta s} = L_{xy s}$	24 mH	$L_{lm}$	11 mH
$L_m$	520 mH	$P$	1

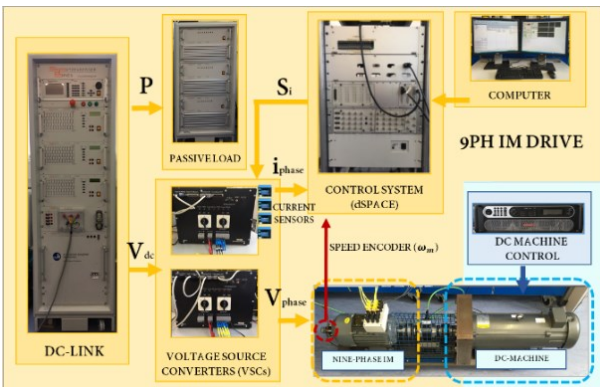


Fig. 4. Test bench including the 1.2 kW nine-phase induction machine.

- Set 1: tests in Figs. 5 and 6 determine the optimum value of  $K_{sw}$  for the SC included in (6).
- Set 2: tests in Figs. 7 and 8 establish the most suitable value of  $C_{sw}$  for the HC included in (8).
- Set 3: tests in Figs. 9 to 11 verify the steady-state and dynamic performance of the proposed MPC with SCs and HCs.

Set 1 compares the standard MPC127 with the MPC that includes the soft constraint (termed from now on MPC-SC). The tests have been done in steady-state condition with a reference speed of 1000 rpm, a  $d$ -current reference of 1.9 A and a load torque of 4 Nm for values of  $K_{sw}$  that range from 0 to 0.25. In order to summarize the most relevant information, Fig. 5 includes the THD of phase currents and the effective switching frequency in the 26 tests. As in any finite-control set MPC, the switching frequency is variable and depends on the switch state that is selected according to the cost function in (6). As expected, the gradual increase of  $K_{sw}$  reduces the switching frequency at the expense of higher THD of the phase currents. It is found however that the slope of the THD rise is rather low for  $K_{sw} \in [0 \dots 0.1]$ , whereas the reduction of the switching frequency is significant.

Taking the MPC127 ( $K_{sw} = 0$ ) and MPC-SC with  $K_{sw} = 0.09$  as two points for comparison, MPC127 has a switching frequency of 2483 Hz, a THD of 26.6% and rms phase currents of 1.607 A, whereas MPC-SC has a switching frequency of 1298 Hz, a THD of 30.3% and rms phase currents of 1.597 A. Hence, the switching frequency is reduced by 48% with a THD increase of 13%. Fig. 6 shows the phase currents from the first set of phase currents ( $a_1 b_1 c_1$ ) when MPC127 (top) and MPC-SC (bottom) methods are used. It can be observed that the deterioration of the current quality is rather low whereas the switching frequency is approximately halved.

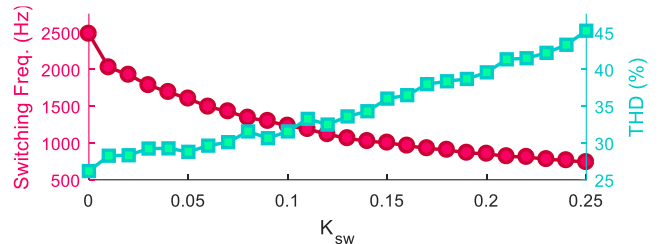


Fig. 5. Switching frequency (red circles, left axis) and phase current THD (green squares, right axis) as a function of the weighting factor  $K_{sw}$  in MPC-SC strategy.

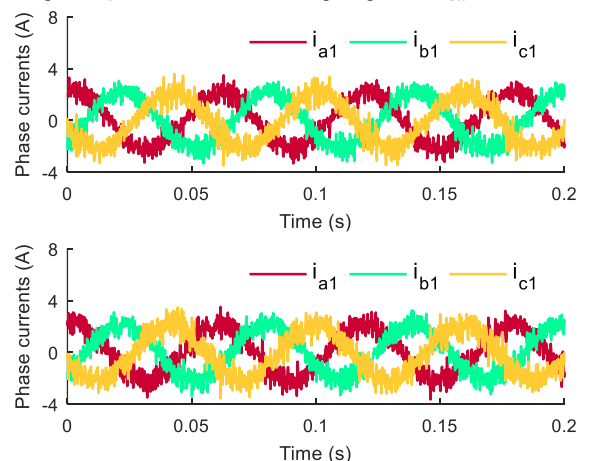


Fig. 6. Measured phase currents of the first three-phase set ( $a_1 b_1 c_1$ ) for MPC127 (i.e.  $K_{sw} = 0$ ; top plots) and MPC-SC strategy with  $K_{sw} = 0.09$  (bottom plots).

The second set of tests (Set 2) has been done to evaluate the goodness of including hard constraints (termed from now on MPC-HC). The operating conditions of this second test are the same as in the first test. MPC-HC with  $C_{sw} \leq 2$  is so restrictive that the performance is extremely poor, hence only cases of  $C_{sw} \in [3 \dots 9]$  have been explored. Fig. 7 again summarizes the switching frequency and THD of phase currents for different values of the threshold  $C_{sw}$ . As in the case of soft constraints, it can be observed that the increasing level of restrictions reduces the switching frequency and worsens the power quality. However, the THD remains mostly constant for  $C_{sw} \geq 5$ , indicating that the discarded vectors are not used by MPC or can be replaced by other vectors with similar performance. Decreasing the threshold  $C_{sw}$  below 5 lowers the switching frequency, but the price to be paid is higher than in the soft approach (e.g. for  $C_{sw} = 4$  the switching frequency is reduced by just 32% and the THD is 19% higher). Although the MPC-SC finds a better balance between switching frequency and THD than MPC-HC, the latter approach provides lower computational cost.

Consequently, a mixture of soft and hard approaches (termed MPC-HSC from now on) can effectively reduce the number of iterations and find optimum balance for low number of commutations with acceptable power quality. Specifically, if  $C_{sw}$  is set to 5 the number of iterations is reduced down to 45 and the performance is very similar to the case when  $C_{sw}$  is set to 9 (see Fig. 8 for a full comparison of both cases). As a main conclusion from testing MPC127, MPC-SC, and MPC-HC, the use of hard constraints is useful to alleviate the computational burden of MPC and the use of soft constraints effectively reduces the switching frequency with very similar current tracking. Specifically, setting  $C_{sw} = 5$  reduces the number of iterations by 64.6% and 91.2% compared to MPC127 and MPC512, respectively, alleviating in this manner the computational requirements for the real time implementation. Furthermore, if  $K_{sw} = 0.09$  then the switching frequency decreases by approximately 50%, confirming that the SC makes use of the inherent redundancies in nine-phase systems (i.e. some switching states provide the same or similar output voltage production). Based on these considerations, the following set of tests (Set 3) will show in detail the performance of the combined MPC-HSC method with  $C_{sw} = 5$  and  $K_{sw} = 0.09$ .

The first test of Set 3 with MPC-HSC is done in steady-state at 1000 rpm, with a  $d$ -current reference of 1.9 A and load torque of 4 Nm (Fig. 9). The speed regulation is satisfactory (Fig. 9a) with well-controlled  $d$ - $q$  currents and values of  $x_1$ - $y_1$  and  $x_2$ - $y_2$  currents around zero (Figs. 9b-9d). Phase currents for the first three-phase set ( $a_1 b_1 c_1$ ) have the expected steady-state sinusoidal values (Fig. 9e). Fig. 9f shows the harmonic spectrum of phase  $a_1$  current. Comparing the MPC-HSC with MPC127, it can be stated that the speed regulation is the same and the current tracking and ripple are mostly similar (Fig. 5), but the computational cost is drastically reduced (65% compared to MPC127 and 90% compared to MPC512) and the switching frequency is 48% lower.

The second test of Set 3 has been done to verify the dynamic performance, by changing the speed reference from 500 to 1250 rpm with load torque of -5Nm (generating mode). Figs. 10a and 10b show correct tracking of the speed and  $d$ - $q$  currents

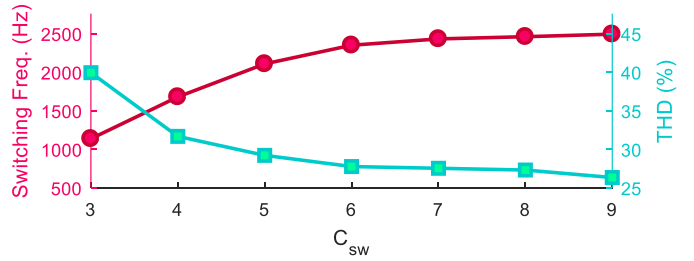


Fig. 7. Switching frequency (red circles, left axis) and phase current THD (green squares, right axis) as a function of the threshold  $C_{sw}$  in MPC-HC strategy.

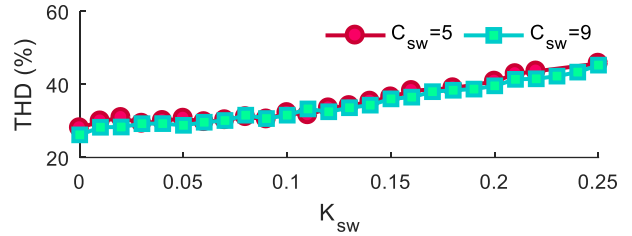


Fig. 8. Phase current THD in MPC-HSC strategy for  $C_{sw} = 9$  (green squares) and  $C_{sw} = 5$  (red circles) as a function of the weighting factor  $K_{sw}$ .

respectively. The  $d$ -current reference is set again to 1.9 A and the  $q$ -current becomes negative (generating mode) and speed-dependent. The  $x_1$ - $y_1$  and  $x_2$ - $y_2$  currents are correctly maintained around zero (Fig. 10c and 10d), proving the correct decoupling between the different planes in dynamic condition. The acceleration of the machine is reflected in the frequency of the  $\alpha$ - $\beta$  and phase currents (Fig. 10e and 10f), which have similar ripple as in the former test.

As the third test of Set 3, a reversal is finally done to further verify the adequacy of performance of the proposed MPC-HSC method. With the same flux setting as in the previous test, the speed command is stepped now from -1000 to 1000 rpm, in motoring mode. It can be observed in Fig. 11a that the machine speed is reversed with acceptable dynamic performance and low overshoot. The  $q$ -current tracking is satisfactory (Fig. 11b), thus confirming the fast response of the MPC approach. Meanwhile, both the  $d$ -current (Fig. 11b) and the secondary currents (11c and 11d) are completely unaltered and close to their target values. Figs. 11e and 11f finally show the transition through zero speed and the inversion of the phase sequence order during the reversal.

## VII. CONCLUSION

Real time implementation of model predictive control in nine-phase drives is challenging, but at the same time the higher number of switching states provides further room for optimization. The analysis of the voltage vectors firstly allows reducing from the initial  $2^9 = 512$  states down to 127. Out of this subset of states, only 45 voltage vectors are evaluated each sampling period after a dynamic selection provided by hard constraints. Soft constraints are finally applied to this second subset of 45 vectors in order to reduce the overall number of commutations. As a result of the state discarding and the use of hard/soft constraints, the proposed MPC-HSC reduces the computational cost and switching frequency by 90% and 50%, respectively, while still maintaining suitable current tracking and dynamic performance.

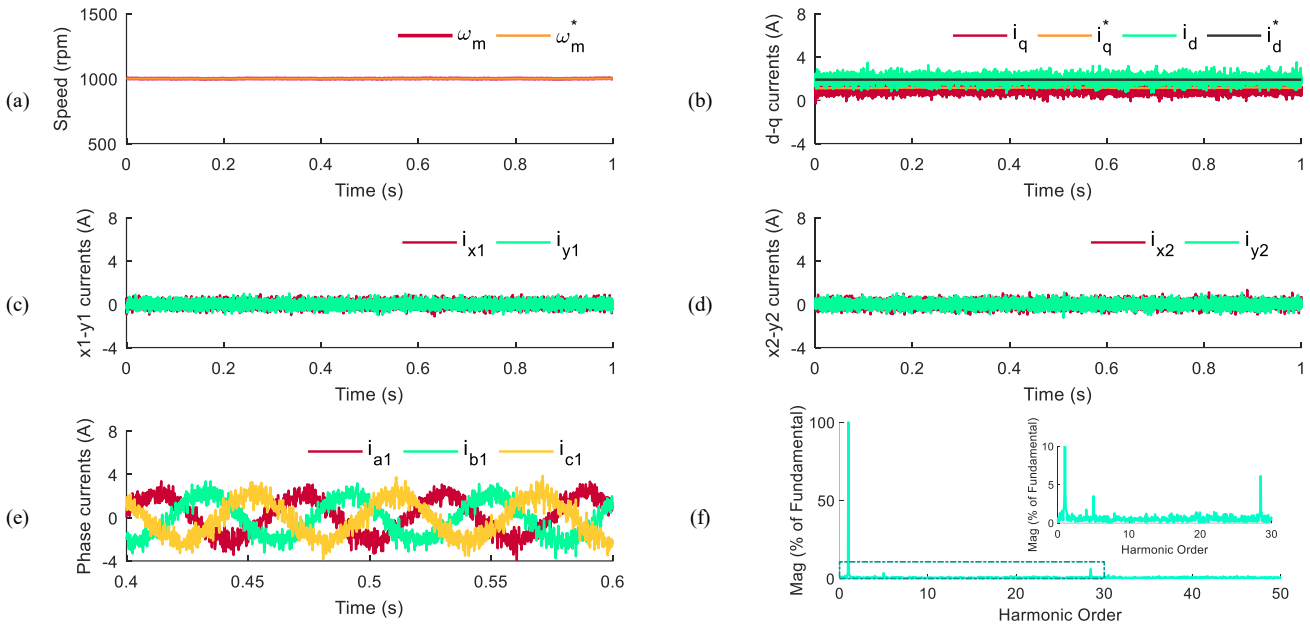


Fig. 9. Steady-state performance of the proposed MPC-HSC: (a) motor speed, (b)  $d$ - $q$  currents, (c)  $x_1$ - $y_1$  currents, (d)  $x_2$ - $y_2$  currents, (e) measured  $a_1 b_1 c_1$  phase currents and (f) spectrum of phase  $a_1$  current.

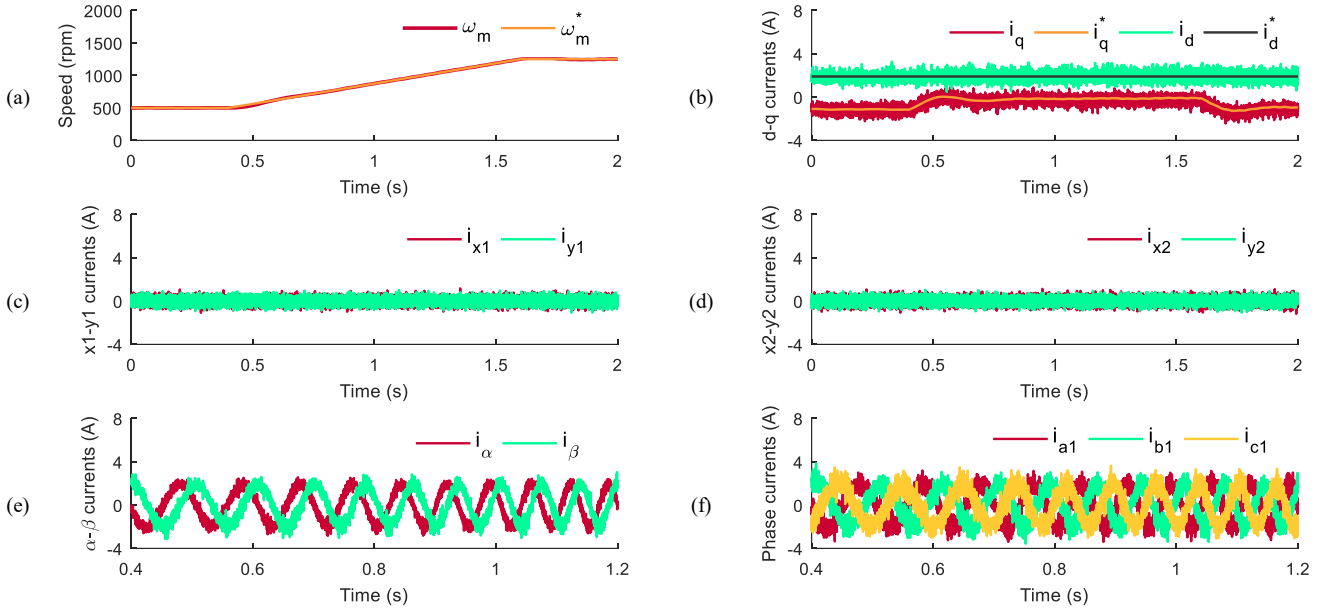


Fig. 10. Dynamic performance (speed ramp reference) of the proposed MPC-HSC: (a) motor speed, (b)  $d$ - $q$  currents, (c)  $x_1$ - $y_1$  currents, (d)  $x_2$ - $y_2$  currents, (e)  $\alpha$ - $\beta$  phase currents and (f) measured  $a_1 b_1 c_1$  phase currents.

## REFERENCES

- [1] S. Vazquez, J. Rodriguez, M. Rivera, L.G. Franquelo and M. Norambuena, "Model predictive control for power converters and drives: Advances and trends," *IEEE Trans. Ind. Electron.*, vol. 64, no. 2, pp. 935-947, 2017.
- [2] Z. Zhang, C.M. Hackl and R. Kennel, "Computationally efficient DMPC for three-level NPC back-to-back converters in wind turbine systems with PMSG," *IEEE Trans. Power Electron.*, vol. 32, no. 10, pp. 8018-8034, 2017.
- [3] I. González-Prieto, M.J. Duran, N. Rios-García, F. Barrero and C. Martín, "Open-switch fault detection in five-phase induction motor drives using model predictive control," *IEEE Trans. Ind. Electron.*, vol. 65, no. 4, pp. 3045-3055, 2018.
- [4] I. Gonzalez-Prieto, M.J. Duran, J.J. Aciego, C. Martin and F. Barrero, "Model predictive control of six-phase induction motor drives using virtual voltage vectors," *IEEE Trans. Ind. Electron.*, vol. 65, no. 1, pp. 27-37, 2018.
- [5] S. Rubino, R. Bojoi, S.A. Odhano and P. Zanchetta "Model predictive direct flux vector control of multi three-phase induction motor drives," *IEEE Trans. Ind. App.*, early access, 2018.
- [6] J. Rodas, C. Martín, M.R. Arahal, F. Barrero and R. Gregor "Influence of Covariance-Based ALS Methods in the Performance of Predictive Controllers With Rotor Current Estimation," *IEEE Trans. Ind. Electron.*, vol. 64, no. 4, pp. 2602-2607, 2017.
- [7] M. Salehifar, J. M. Moreno-Eguilaz, J. M. Moreno-Eguilaz, G. Putrus and Peter Barras, "Simplified fault tolerant finite control set model predictive control of a five-phase inverter supplying BLDC motor in electric vehicle drive," *Electric Power Systems Research*, vol. 132, pp. 56-66, DOI: 10.1016/j.epsr.2015.10.030.
- [8] S. Kouro, P. Cortes, R. Vargas, U. Ammann and J. Rodriguez, "Model Predictive Control—A Simple and Powerful Method to Control Power Converters," *IEEE Trans. Ind. Electron.*, vol. 56, no. 6, pp. 1826-1838, 2009.

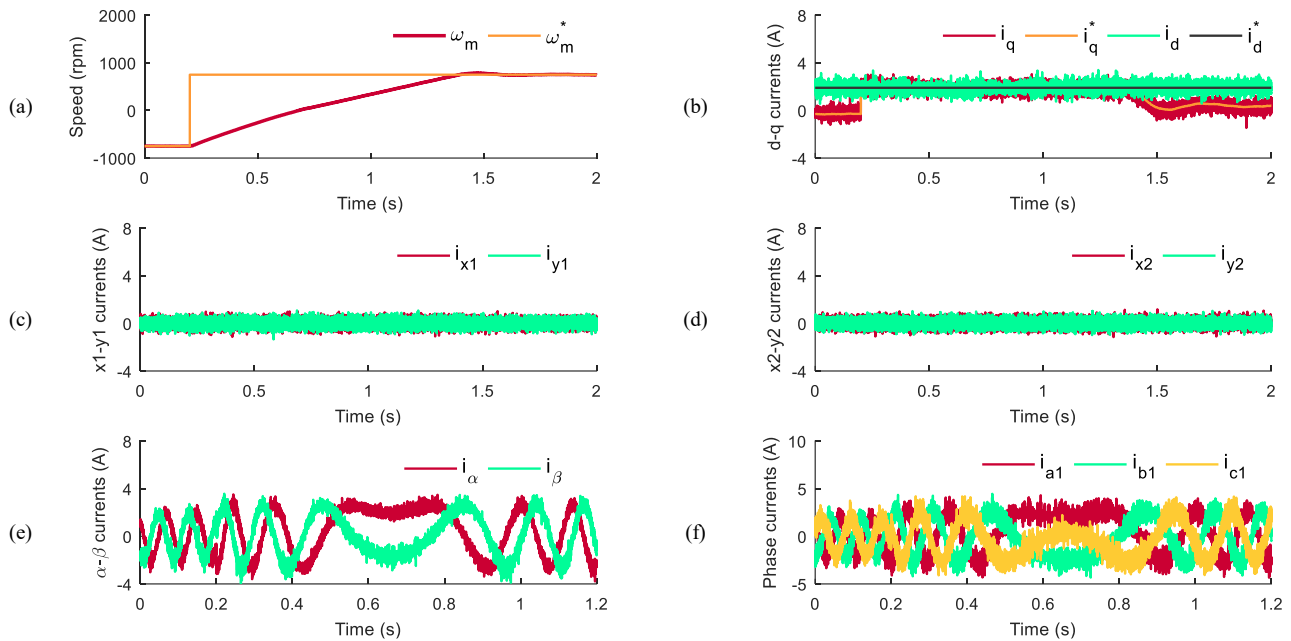


Fig. 11. Dynamic performance (speed reversal) of the proposed MPC-HSC: (a) motor speed, (b)  $d$ - $q$  currents, (c)  $x_1$ - $y_1$  currents, (d)  $x_2$ - $y_2$  currents, (e)  $\alpha$ - $\beta$  phase currents and (f) measured  $a_1 b_1 c_1$  phase currents.

- [9] H.A. Young, M.A. Perez, J. Rodriguez and H. Abu-Rub, "Assessing Finite-Control-Set Model Predictive Control: A Comparison with a Linear Current Controller in Two-Level Voltage Source Inverters," *IEEE Ind. Electron. Magazine*, vol. 8, no. 1, pp. 44-52, 2014.
- [10] Y. Zhang, B. Xia and H. Yang, "Performance evaluation of an improved model predictive control with field oriented control as a benchmark," *IET Electric Power App.*, vol. 11, no. 5, pp. 677-687, 2017.
- [11] C.S. Lim, E. Levi, M. Jones, N.A. Rahim and W.P. Hew, "FCS-MPC-based current control of a five-phase induction motor and its comparison with PI-PWM control," *IEEE Trans. Ind. Electron.*, vol. 61, no. 1, pp. 149-163, 2014.
- [12] C.S. Lim, E. Levi, M. Jones, N.A. Rahim and W.P. Hew, "A Comparative Study of Synchronous Current Control Schemes Based on FCS-MPC and PI-PWM for a Two-Motor Three-Phase Drive," *IEEE Trans. on Ind. Electron.*, vol. 61, no. 8, pp. 3867-3878, 2014.
- [13] H. Guzman, M.J. Duran, F. Barrero, L. Zari, B. Bogado, I. Gonzalez-Prieto and M.R. Arahal, "Comparative Study of Predictive and Resonant Controllers in Fault-Tolerant Five-Phase Induction Motor Drives," *IEEE Trans. Ind. Electron.*, vol. 63, no. 1, pp. 606-617, 2016.
- [14] M. J. Duran, J. A. Riveros, F. Barrero, H. Guzman and J. Prieto, "Reduction of Common-Mode Voltage in Five-Phase Induction Motor Drives Using Predictive Control Techniques," *IEEE Trans. Ind. App.*, vol. 48, no. 6, 2012.
- [15] E. Levi, F. Barrero and M.J. Duran, "Multiphase machines and drives – Revisited," *IEEE Trans. Ind. Electron.*, vol. 63, no. 1, pp. 429-432, 2016.
- [16] E. Levi, "Advances in converter control and innovative exploitation of additional degrees of freedom for multiphase machines," *IEEE Trans. Ind. Electron.*, vol 63, no. 1, pp. 433-448, 2016.
- [17] F. Barrero and M.J. Duran, "Recent advances in the design, modeling and control of multiphase machines – Part 1," *IEEE Trans. Ind. Electron.*, vol 63, no. 1, pp. 449-458, 2016.
- [18] F. Barrero, M.R. Arahal, R. Gregor, S. Toral and M.J. Duran, "A proof of concept study of predictive current control for VSI driven asymmetrical dual three-phase AC machines," *IEEE Trans. Ind. Electron.*, vol. 56, no. 6, pp. 1937-1954, 2009.
- [19] M.J. Duran, J. Prieto, F. Barrero and S. Toral, "Predictive current control of dual three-phase drives using restrained search techniques," *IEEE Trans. Ind. Electron.*, vol. 58, no. 8, pp. 3253-3263, 2011.
- [20] R. Vargas, P. Cortes, U. Ammann, J. Rodriguez, and J. Pontt, "Predictive control of a three-phase neutral-point-clamped inverter," *IEEE Trans. Ind. Electron.*, vol. 54, no. 5, pp. 2697-2705, Oct. 2007.
- [21] M.J. Duran, E. Levi and F. Barrero, *Multiphase Electric Drives: Introduction*, Wiley Encyclopedia of Electrical and Electronics Engineering, pp. 1-26, 2017.
- [22] E. Jung, H. Yoo, S. Sul, H. Choi and Y. Choi, "A nine-phase permanent-magnet motor drive system for an ultrahigh-speed elevator," *IEEE Trans. Ind. Appl.*, vol. 48, no. 3, pp. 987-995, 2012.
- [23] A.S. Abdel-Khalik, M.S. Hamad, A.M. Massoud and S. Ahmed, "Postfault operation of a nine-phase six-terminal induction machine under single open-line fault," *IEEE Trans. Ind. Electron.*, vol. 65, no. 2, pp. 1084-1096, 2018.
- [24] I. Subotic, N. Bodo, E. Levi and M. Jones, "Onboard integrated battery charger for EVs using an asymmetrical nine-phase machine," *IEEE Trans. Ind. Electron.*, vol 62, no. 5, pp. 3285-3295, 2015.
- [25] I. Zoric, M. Jones and E. Levi, "Arbitrary Power Sharing Among Three-Phase Winding Sets of Multiphase Machines," *IEEE Trans. Ind. Electron.*, vol 65, no. 2, pp. 1128-1139, 2018.
- [26] M. Cheng, F. Yu, K.T. Chau and W. Hua, "Dynamic performance evaluation of a nine-phase flux-switching permanent-magnet motor drive with model predictive control," *IEEE Trans. Ind. Electron.*, vol. 63, no. 7, pp. 4539-4549, 2016.



**Ignacio González Prieto** was born in Malaga, Spain, in 1987. He received the Industrial Engineer and M.Sc. degrees in fluid mechanics from the University of Malaga, Malaga, Spain, in 2012 and 2013, respectively, and the Ph.D. degree in electronic engineering from the University of Seville, Sevilla, Spain, in 2016. His research interests include multiphase machines, wind energy systems, and electrical vehicles



**Ivan Zoric** (S'17) received the BSc and MSc degrees in Electrical Engineering from the University of Belgrade, Serbia in 2010 and 2013, respectively. He joined in June 2014 Liverpool John Moores University, UK, as a PhD student. He completed his PhD in electrical engineering in April 2018 and is since with Dyson. His main research interests include power electronics and advanced machine drives.



**Mario J. Duran** was born in Bilbao, Spain, in 1975. He received the M.Sc. and Ph.D. degrees in electrical engineering from the University of Malaga, Malaga, in 1999 and 2003, respectively. He is currently a Full Professor in the Department of Electrical Engineering, University of Malaga. His research interests include modeling and control of multiphase drives and renewable energies conversion systems.



**Emil Levi** (S'89, M'92, SM'99, F'09) received his MSc and the PhD degrees in Electrical Engineering from the University of Belgrade, Yugoslavia in 1986 and 1990, respectively. He joined Liverpool John Moores University, UK in May 1992 and is since September 2000 Professor of Electric Machines and Drives. He served as a Co-Editor-in-Chief of the IEEE Trans. on Industrial Electronics in the 2009-2013 period and is currently Editor-in-Chief of the

IET Electric Power Applications, Editor-in-Chief of the IEEE Trans. on Industrial Electronics, and an Editor of the IEEE Trans. on Energy Conversion. He is the recipient of the Cyril Veinott award of the IEEE Power and Energy Society for 2009 and the Best Paper award of the IEEE Trans. on Industrial Electronics for 2008. In 2014 he received the "Outstanding Achievement Award" from the European Power Electronics (EPE) Association and in 2018 the "Professor Istvan Nagy Award" from the Power Electronics and Motion Control (PEMC) Council.